

EFFECTS OF FIXTURE DYNAMICS ON BACK-STEPPING CONTROL OF A VR SPHERICAL MOTOR

Kok-Meng Lee

Georgia Institute of Technology
George W. Woodruff School of Mechanical Eng.
Atlanta, GA 39332-0405

Raye A. Sosseh

Seagate Technologies
Servo Engineering Technology
Oklahoma City, OK 73134

ABSTRACT

This paper presents the effects of fixture dynamics on the control of a variable-reluctance spherical motor (VRSM). The cascaded VRSM dynamics has the appropriate structure for the so-called back-stepping controller design method. Implementation of the back-stepping controller, however, requires the computation of the exact motor dynamics at each sampling time. This computational burden has an effect on the performance of the control algorithm and imposes constraints on the hardware/software architecture of the control system. By only computing the dominant parts of the motor dynamics, this computational burden can be reduced. We have developed a robust back-stepping controller to compensate for uncertainties account for imperfect modeling and intentional computational simplification. The performance of the robust back-stepping controller has been evaluated experimentally against a classical PD controller and a standard back-stepping controller, which serve as bases for comparison.

1. INTRODUCTION

Multi-degree-of-freedom (DOF) actuators are finding wide uses in a number of industries. For high precession trajectory planning and control, it is desired to replace the actuator system made up of several single-DOF motors connected in series and/or parallel with a dexterous spherical multi-DOF actuator. The need for such systems has motivated years of research in the development of unusual, yet high performance actuators that have the potential to realize multi-DOF motion in a single joint. One such actuator is the spherical motor. Compared to conventional robotic manipulators that offer the same motion capabilities, the spherical motor possesses several advantages much simpler and more compact in design.

A brief review of prior research efforts on the spherical motors can be found in [1]. Of particular interest here is the development of a VRSM, where earlier works have been largely focused on the understanding of the operating principles, deriving the torque model, and developing the design/control methodology. Most of these studies have largely ignored the loading effects on the performance. The dynamics of fixtures and tooling that are mounted on the multi-DOF actuator may not be neglected for high-precision applications. For this reason, we have developed a robust back-stepping controller and examined the effects of the fixture or tooling dynamics on the VRSM controlled system using an existing setup.

The cascaded VRSM dynamics has the appropriate structure for the so-called back-stepping controller design method. Kokotovic [2] published one of the pioneering works

on the back-stepping control technique and Qu *et al.* [3] extended this technique and developed a robust back-stepping-type controller for a one-link robot with the motor dynamics taken into consideration. Carroll *et al.* [4] also extended the work of Kokotovic [2] to design an embedded computed torque and output feedback controller for permanent magnet brush dc (BDC) motors. Hemati *et al.* [5] developed a robust feedback linearizing controller for a single-link robot actuated by a brushless dc motor (BLDC). In [6], Carroll *et al.* also developed a robust tracking controller for a BLDC, which achieved globally bounded results for rotor position tracking error despite parametric uncertainties and additive bounded disturbances. Unlike prior works that the back-stepping controllers have been applied to the control of numerous single-axis machines and serial or parallel robotic mechanisms, we investigate the back-stepping control design in the context of a VRSM with the ability to compensate for model imperfections.

The remainder of this paper is organized as follows. Section 2 begins with the presentation of the system dynamics and the torque model of a VR spherical motor, along with constraints imposed by a fixture. The formulation of the control problem is given in Section 3, where the design of the back-stepping-type controller using Lyapunov-type stability arguments is presented. The performances of the two back-stepping controllers, with and without a robust term, are compared in Section 4. Finally, the conclusions are given in Section 5.

2. SYSTEM MODEL

The VRSM referred to in this paper has a similar structure as ball-joint-like device in [7]. Clearly, this specific structure is chosen here for the purpose of illustrating the effects of tooling dynamics on the control of a VR spherical motor and because a prototype of such a structure has been available for experimental verification. Extension of the techniques for other forms of fixtures, tooling or payload dynamics is expected to be relatively straight-forward.

As shown in Figure 1, the structure is made up of four basic assemblies, a spherical rotor, a hollow spherical stator, a bearing system, and an orientation measurement system. The stator houses a number of electromagnets strategically distributed on the inside of its surface. Similarly, the rotor consists of a number of poles made up of ferromagnetic materials or permanent magnets. Feedback control of the spherical motor requires an orientation measurement system. When off-the-shelf single-axis encoders are used, a typical orientation measurement system requires a mechanism that consists of the two arc-shaped guides and a sliding block. The

two guides are mounted orthogonally on bearing pins attached to the outside of the stator for measuring the rotation of their corresponding guides. The Z encoder measures the spin of the rotor shaft about its axis. Detailed derivations of the kinematics that relate the encoder readings $(\theta_x, \theta_y, \theta_z)$ to the rotor orientation or the ZYZ Euler angles (ψ, θ, ϕ) can be found in [8]. The measuring system contributes to two-thirds of the total system inertia and can not be neglected.

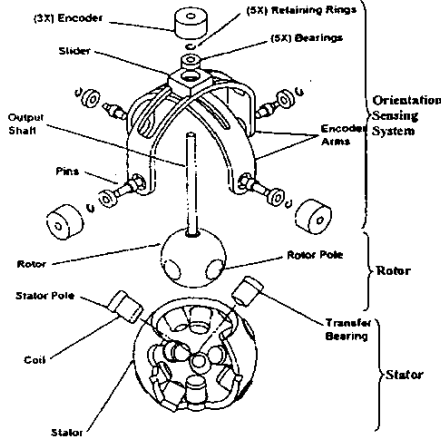


Figure 1 Exploded view of a VRSM CAD model

2.1 Rotor and Tooling Dynamics

The effects of the X- and Y-guides on the rotor dynamics can be described by the constraint equations in the following form:

$$f_1(\mathbf{q}^T; \theta_x, \theta_y) = 0 \quad (1a)$$

$$f_2(\mathbf{q}^T; \theta_x, \theta_y) = 0 \quad (1b)$$

where \mathbf{q} is a 3x1 vector of the ZYZ Euler angles; and (θ_x, θ_y) are angular displacement measured about x-axis and y-axis respectively. In order to include the constraints imposed by the X- and Y-guides, we use a Lagrange formulation to derive the dynamic model for the combined rotor and encoder mechanism.

$$\frac{d}{dt} \left(\frac{\partial \mathbf{L}}{\partial \dot{\mathbf{q}}_j} \right) - \frac{\partial \mathbf{L}}{\partial \mathbf{q}_j} = \mathbf{Q}_j + \sum_{i=1}^2 a_{ij} \lambda_i \quad (2)$$

where $j = 1, \dots, 5$; \mathbf{L} is Lagrangian; \mathbf{Q}_j represents the applied torque; λ_1 and λ_2 are constrained Lagrange multipliers; and the term $\sum_{i=1}^2 a_{ij} \lambda_i$ represents the contribution of the reaction forces (from the measurement guides) to the generalized moments. In Equation (2), a_{ij} are the elements of the Jacobian matrix $[\mathbf{a}] = \begin{bmatrix} \mathbf{a}_r \\ \mathbf{I}_2 \end{bmatrix}$ of the angular velocity constraints, which can be derived by differentiating Equations (1a) and (1b), in the following form:

$$\begin{bmatrix} \mathbf{a}_r \\ \mathbf{I}_2 \end{bmatrix} \begin{bmatrix} \mathbf{q} \\ \theta_x \\ \theta_y \end{bmatrix} = \begin{bmatrix} 0 \\ 0 \end{bmatrix}$$

where $[\mathbf{a}_r]$ is a 3x2 matrix the elements of which are functions of the ZYZ Euler angles; and $[\mathbf{I}_2]$ is a 2x2 identity matrix. It can be shown that the dynamic model of the combined rotor/sensor mechanism can be written in the following compact form:

$$[\mathbf{H}(\mathbf{q})]\ddot{\mathbf{q}} + \mathbf{C}(\mathbf{q}, \dot{\mathbf{q}}) = [\mathbf{B}(\mathbf{q})]\mathbf{T}(\mathbf{q}) \quad (3)$$

$$\text{where } [\mathbf{H}(\mathbf{q})] = [\mathbf{J}_r] + [\mathbf{a}_r^T][\mathbf{J}_g][\mathbf{a}_r] \quad (3a)$$

$$[\mathbf{C}(\mathbf{q}, \dot{\mathbf{q}})] = \boldsymbol{\tau} + [\mathbf{a}_r^T][\mathbf{J}_g][\dot{\mathbf{a}}_r] \quad (3b)$$

$$[\mathbf{B}(\mathbf{q})] = \begin{bmatrix} -S_\theta C_\theta & S_\theta S_\theta & C_\theta \\ S_\theta & C_\theta & 0 \\ 0 & 0 & 1 \end{bmatrix} \quad (3c)$$

$$[\mathbf{J}_r] = \begin{bmatrix} (I_2 - I_1) \cos^2 \theta + I_1 & 0 & I_2 \cos \theta \\ 0 & I_1 & 0 \\ I_2 \cos \theta & 0 & I_2 \end{bmatrix} \quad (3d)$$

$$[\mathbf{J}_g] = \begin{bmatrix} I_{Xg} & 0 \\ 0 & I_{Yg} \end{bmatrix} \quad (3e)$$

$$[\mathbf{a}_r] = \begin{bmatrix} -S_\theta C_\theta C_\psi & -S_\psi & 0 \\ S_\theta^2 S_\psi^2 + C_\theta^2 & S_\theta^2 S_\psi^2 + C_\theta^2 & 0 \\ S_\theta C_\theta C_\psi & -C_\psi & 0 \\ S_\theta^2 C_\psi^2 + C_\theta^2 & S_\theta^2 C_\psi^2 + C_\theta^2 & 0 \end{bmatrix} \quad (3f)$$

$$\text{and } \boldsymbol{\tau} = \begin{bmatrix} 2(I_2 - I_1)S_\theta C_\theta \psi \dot{\theta} + I_2 S_\theta \dot{\theta} \dot{\psi} \\ (I_1 - I_2)S_\theta C_\theta \psi^2 - I_2 S_\theta \psi \dot{\psi} \\ I_2 S_\theta \psi \dot{\theta} \end{bmatrix} \quad (3g)$$

2.2 Torque Model

The torque generated by the spherical motor is typically quadratic and has the following form:

$$T_l = \frac{1}{2} \mathbf{I}_s^T \frac{\partial [L_{ss}]}{\partial \theta_l} \mathbf{I}_s + \frac{1}{2} \mathbf{I}_r^T \frac{\partial [L_{rr}]}{\partial \theta_l} \mathbf{I}_r + \mathbf{I}_r^T \frac{\partial [L_{sr}]}{\partial \theta_l} \mathbf{I}_s \quad (4)$$

where \mathbf{I}_s and \mathbf{I}_r are the stator and rotor current input vectors respectively; $[L_{ss}]$ and $[L_{rr}]$ are the self-inductance sub-matrices of the stator and rotor respectively; and $[L_{sr}] = [L_{rs}]^T$ is the mutual inductance sub-matrix. The specific form of the torque depends on the structure of the motor. For a configuration where coils are wound on non-ferromagnetic cores and permanent magnets are used as rotor poles, the third term in Equation (4) is eliminated. In addition, the self-inductance term is small compared to the second term due to mutual-inductance term. Thus, the torque can be approximated by a linear combination of stator input currents:

$$T_l = \mathbf{I}_r^T \frac{\partial [L_{sr}]}{\partial \theta_l} \mathbf{I}_s = [\mathbf{K}(\mathbf{q})] \mathbf{u} \quad (5)$$

where $\mathbf{K}_l(\mathbf{x}_1) \in R^{3 \times n}$ is the torque constant matrix; $\mathbf{u} \in R^n$ is the control vector of stator coil currents; n is the number of stator

coils; and $q = [\psi, \theta, \phi]^T$ is a vector of ZYZ Euler angles describing the rotor orientation w. r. t. the stator reference frame.

For a specified torque, the current input vector is found by minimizing the control input energy consumption

$$J = \frac{1}{2} \mathbf{u}^T [W] \mathbf{u} \quad (6)$$

where $[W] \in R^{10 \times 10}$ is a positive definite weighting matrix, subject to the desired torque constraint given by Equation (12). Provided that the control currents are kept within limits, the optimal solution to this problem can be solved using Lagrange multipliers. The optimal solution can be written in closed form:

$$\mathbf{u} = [W]^{-1} [K_1^T] \left[[K_1] [W]^{-1} [K_1^T] \right]^{-1} \mathbf{T} \quad (7)$$

2. FORMULATION OF VRSM CONTROL

The control objective for the spherical motor is to move the rotor from an initial state to a specified final state, while minimizing the system energy consumption. The spherical motor control objective can therefore be stated as follows: Given the constraint Lagrange equations:

$$\dot{\mathbf{x}}_1 = \mathbf{x}_2 \quad (8)$$

$$[H(\mathbf{x}_1)] \dot{\mathbf{x}}_2 = \mathbf{T}(\mathbf{x}_1, \mathbf{u}) - \mathbf{C}(\mathbf{x}_1, \mathbf{x}_2) \quad (9)$$

where $\mathbf{x}_1 = \mathbf{q}$ is a 3x1 vector of the ZYZ Euler angles (ψ, θ, ϕ) ,

\mathbf{x}_2 is the corresponding angular velocities,

$[H(\mathbf{x}_1)]$ is a symmetric, positive-definite inertia matrix,

and $\mathbf{C}(\mathbf{x}_1, \mathbf{x}_2)$ represents the vector of coriolis terms,

the control problem is to determine the sub-optimal control vector \mathbf{u} that will drive the rotor from its initial state to a specified final state while minimizing the cost function given by Equation (6).

The controller developed is designed in two parts. The desired torque required to stabilize the system is first derived. In the second part, the current inputs required to generate the desired torque is determined from the solution of a static optimization given by Equation (7).

3.2 Back-stepping Controller

The cascaded spherical motor dynamics in Equations (8) and (9) have the appropriate structure for the back-stepping controller design method. The desired torque for a back-stepping controller has the following form:

$$\mathbf{T}_d = [H] \mathbf{y} + \mathbf{C}(\mathbf{x}_1, \mathbf{x}_2) \quad (10)$$

Equation (10) is a nonlinear compensator since it depends on the dynamics of the spherical motor, where \mathbf{y} is derived such that the rotor will track the desired specified state \mathbf{x}_{1d} if the position error dynamics are given as follows:

$$\dot{\mathbf{z}}_1 + [K_p] \mathbf{z}_1 = 0 \quad (11)$$

where $\mathbf{z}_1 = \mathbf{x}_{1d} - \mathbf{x}_1$; and

$[K_p]$ is a positive definite gain matrix.

Equation (11) can be rewritten as

$$\mathbf{x}_2 = \dot{\mathbf{x}}_{1d} + [K_p] \mathbf{z}_1 \quad (11a)$$

Substituting the fictitious control input \mathbf{x}_{2d} for \mathbf{x}_2 in Equation (11a) yields

$$\mathbf{x}_{2d} = \dot{\mathbf{x}}_{1d} + [K_p] (\mathbf{x}_{1d} - \mathbf{x}_1) \quad (12)$$

The fictitious control input \mathbf{x}_{2d} is selected as the specified velocity trajectory leading to the velocity error:

$$\mathbf{z}_2 = \mathbf{x}_{2d} - \mathbf{x}_2$$

The error dynamics in Equation (13) ensures the velocity error approaches zero asymptotically, which will eventually lead to the asymptotic convergence of the rotor position error.

$$\dot{\mathbf{z}}_2 + [K_d] \mathbf{z}_2 = 0 \quad (13)$$

where $[K_d]$ is a positive-definite gain matrix. Equation (13) can be rewritten as

$$\dot{\mathbf{x}}_2 = \dot{\mathbf{x}}_{2d} + [K_d] \mathbf{z}_2 \quad (13a)$$

Substituting Equation (13a) into Equation (9) leads to the stabilizing torque:

$$\mathbf{T}_a = [H](\dot{\mathbf{x}}_{2d} + [K_d] \mathbf{z}_2) + \mathbf{C}(\mathbf{x}_1, \mathbf{x}_2) \quad (14)$$

Comparing Equation (14) and Equation (10) leads to

$$\mathbf{y} = \dot{\mathbf{x}}_{1d} + [K_p] (\mathbf{x}_{1d} - \mathbf{x}_1) + [K_d] \left\{ [\mathbf{x}_{1d} + [K_p] (\mathbf{x}_{1d} - \mathbf{x}_1)] - \dot{\mathbf{x}}_1 \right\}$$

or

$$\mathbf{y} = \dot{\mathbf{x}}_{1d} + ([K_p] + [K_d]) (\mathbf{x}_{1d} - \mathbf{x}_1) + [K_p] [K_d] (\mathbf{x}_{1d} - \mathbf{x}_1) \quad (15)$$

3.3 Robust Back-Stepping Controller

To account for the uncertainties in the spherical motor dynamics, the controller takes the following form:

$$\mathbf{T}_a = [\hat{H}] \mathbf{y} + \hat{\mathbf{C}} \quad (16)$$

$$\mathbf{y} = \dot{\mathbf{x}}_{1d} + ([K_p] + [K_d]) \mathbf{z}_2 + ([K_p] [K_d]) \mathbf{z}_1 + \mathbf{w} \quad (17)$$

where $[\hat{H}]$ and $\hat{\mathbf{C}}$ are the estimated inertia and coriolis terms in the VRSM dynamics; and the proper choice of robust term \mathbf{w} will ensure the stability of the system even in the presence of uncertainties.

Error Dynamics in the Presence of Uncertainties

Application of the robust controller in Equations (16) to the spherical motor dynamics in Equations (8) and (9) leads to the following closed loop dynamics:

$$[H] \dot{\mathbf{x}}_2 + \mathbf{C} = [\hat{H}] \mathbf{y} + \hat{\mathbf{C}} \quad (18)$$

Since the inertia matrix $[H]$ is symmetric and positive definite, the closed loop dynamics in Equation (9) can be rewritten as

$$\dot{\mathbf{x}}_1 = \mathbf{y} - \boldsymbol{\eta} \quad (19)$$

where $\boldsymbol{\eta} = ([I] - [H]^{-1} [\hat{H}]) \mathbf{y} - [H]^{-1} (\hat{\mathbf{C}} - \mathbf{C})$ (19a)

Substitution of Equation (17) for \mathbf{y} into Equation (19) results in the following expression for the closed loop error dynamics:

$$\dot{\tilde{\mathbf{x}}}_1 + ([K_p] + [K_d]) \tilde{\mathbf{x}}_1 + [K_p] [K_d] \tilde{\mathbf{x}}_1 = \boldsymbol{\eta} - \mathbf{w}$$

which can be rewritten as

$$\dot{\tilde{\boldsymbol{\xi}}} = [\tilde{F}] \tilde{\boldsymbol{\xi}} + [D] (\boldsymbol{\eta} - \mathbf{w}) \quad (20)$$

where $\tilde{\boldsymbol{\xi}} = \begin{bmatrix} \tilde{\mathbf{x}}_1 \\ \dot{\tilde{\mathbf{x}}}_1 \end{bmatrix} = \begin{bmatrix} \mathbf{x}_{1d} - \mathbf{x}_1 \\ \dot{\mathbf{x}}_{1d} - \dot{\mathbf{x}}_1 \end{bmatrix}$; (20a)

$[\tilde{F}] = \begin{bmatrix} [0] & [I] \\ -[K_1] & -[K_2] \end{bmatrix}$ is a block matrix of dimension $R^{6 \times 6}$; and

$[D] = \begin{bmatrix} [0] \\ [I] \end{bmatrix}$ and $[K] = \begin{bmatrix} [K_1] \\ [K_2] \end{bmatrix} = \begin{bmatrix} [K_p] [K_d] \\ [K_p] + [K_d] \end{bmatrix}$ are of dimension

To avoid the singularity that results from the simulation of the robust controller given by Equations (17) and (26), the following modification to the robust term.

$$w = \begin{cases} \frac{\rho}{\|z\|} z & \|z\| \geq \epsilon \\ \frac{\rho}{\epsilon} z & \|z\| < \epsilon \end{cases}$$

Test Case 1

The spherical motor is commanded to move from its initial state $(0^\circ, 0^\circ, 0^\circ)$ to a final state $(0^\circ, 10^\circ, 60^\circ)$, which corresponds to a 10° inclination of the Y -encoder guide and a 60° spin of the rotor shaft. The simulation and experimental results for the robust back-stepping control of the spherical motor are compared in Figure 4. The controller gains are $[K_p] = \text{diag}(10, 30, 40)$ and $[K_d] = \text{diag}(12, 45, 12.5)$.

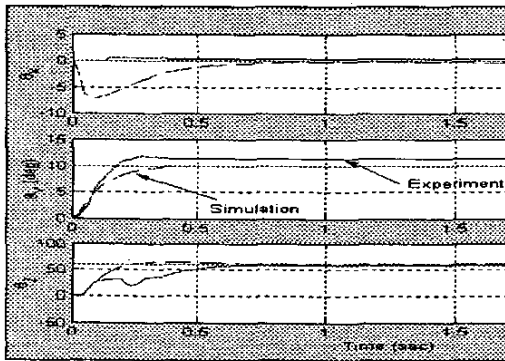


Figure 4: Robust Back-stepping Control (Test case 1)

As a basis for comparison, the performance of the robust back-stepping controller is evaluated against a PD controller, where the controller gains are tuned with the aid of simulation. As compared in Figure 5, a properly tuned PD controller performs as well as the back-stepping-type controller for point to point control.

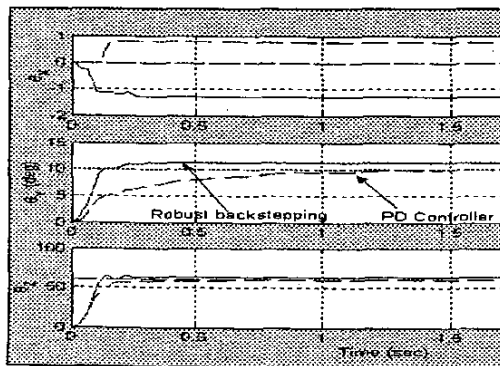


Figure 5: Comparison against PD Controller

Figure 6 compares the performance of the back-stepping control with and without the robust term. The performances, with and without the robust terms, are close. The dynamic model of the back-stepping controller is apparently reasonably

good. The robust back-stepping controller, however, has a slightly faster response time. The primary advantage of the back-stepping controller over the PD controller is the ability to track time varying inputs.

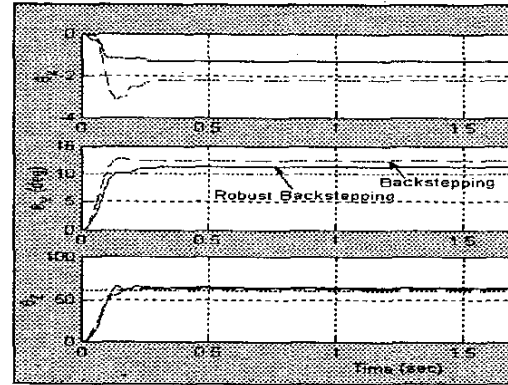


Figure 6: Effect of the Robust Term

Test Case 2

Two consecutive motions are involved. The spherical motor is first commanded to move from its initial position $(0^\circ, 0^\circ, 0^\circ)$ to an intermediate state that is essentially a 10° inclination of the Y -encoder guide or $(0^\circ, 10^\circ, 80^\circ t)$, while maintaining a shaft spin rate of 80° . In the second stage, while maintaining the same spin rate as in the first stage, the spherical motor is commanded to move to a final state of $(0^\circ, 2^\circ, 60^\circ t)$. Figure 6 shows the response of the spherical motor with the robust back-stepping-type controller. As shown in Figure 7, the back-stepping-type controller has performed very satisfactorily. Experimental results have shown that a PD controller would exhibit unstable behaviors for time-varying trajectory following.

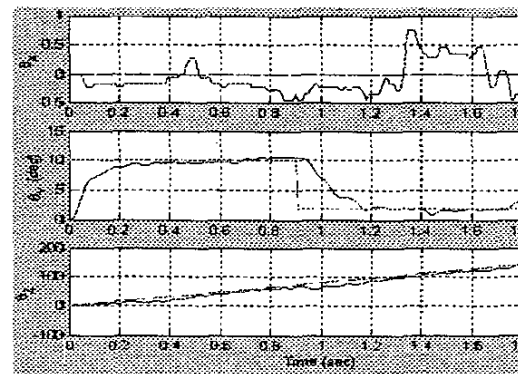


Figure 7: Robust Back-stepping Tracking Control (Test Case 2)

The desired and applied current inputs are shown in Figures 8(a) and (b) respectively. The corresponding torque components are shown in Figure 9. It is also observed that the currents in stator coils 6 through 10 are equal but opposite in direction to the currents in coils 1 through 5. This current input configuration results directly from the solution of the torque-to-current optimization problem. The current excitation pattern is

due to the symmetric arrangement of the spherical motor coils. The desired currents were within the current limit for most part of the response. The desired and applied torque components were therefore equivalent.

5. CONCLUSIONS

A detailed dynamic model of a VR spherical motor, along with the method of incorporating the constraints imposed by the fixtures, tooling or payload in the derivation of the VRSM dynamics, has been presented. The robust back-stepping controller presented here provides an effective means to compensate for uncertainties accountable for imperfect modeling and intentional computational simplification.

The performances of two back-stepping controllers, with and without a robust term, have been evaluated experimentally against a PD controller that serves as a basis for comparison. The performances of the back-stepping controller, with and without the robust terms, are close, which implies that the dynamic model incorporating the constraints imposed by the fixture is apparently good. The robust back-stepping controller, however, has a slightly faster response time. The primary advantage of a back-stepping controller over the PD controller is its ability to track time varying inputs.

Preliminary results in this paper are promising. The techniques can be extended to account for other forms of fixtures, tooling or payload dynamics.

ACKNOWLEDGEMENT

The authors thank Debao Zhou and Jeffery Joni for their assistance in developing the prototype rotor used in this paper.

REFERENCES

- [1] Lee, K.-M. and R. Soseh, "Effects of the Torque Model on the Control of a VR Spherical Motor," *Proc. the 2nd IFAC Mechatronics*, December 2002, San Francisco, CA.
- [2] Kokotovic, P., "The Joy of feedback: nonlinear and adaptive," *IEEE Control System Magazine*, vol. 12, pp. 7-17, June, 1992.
- [3] Qu, Z., and D. M. Dawson, "Lyapunov direct design of robust tracking control for classes of cascaded nonlinear uncertain systems without matching conditions," *Proc. of the 30th IEEE CD C*, Brighton, UK, 1991, vol. 3, pp. 2521-2526.
- [4] Carroll, J. J., and D. M. Dawson, "Integrator backstepping techniques for the tracking control of permanent magnet brush DC motors," *IEEE Trans. on Industry Applications*, Vol. 31, no. 2, Mar.-Apr. 1995, pp. 248-255
- [5] Hemati, N., J. Thorp, J., and M. Leu, "Robust nonlinear control of brushless dc motors for direct-drive robotic applications," *IEEE Trans. on Ind. Electronics*, vol. 37, no. 6 pp. 460-468, Dec., 1990.
- [6] Carroll, J., and D. M. Dawson, "Robust tracking control of a brushless dc motor with application to robotics," *Proc. IEEE ICRA*, Atlanta, GA., pp. 94-99, May, 1993.
- [7] Lee, K.-M., R. Roth, and Z. Zhou, "Dynamic Modeling and Control of a Ball-joint-like VR Spherical Motor," *ASME J. Dyn. Sys., Meas. and Control*, vol. 118, no. 1, pp. 29-40, March 1996.
- [8] Lee, K.-M. and J. Pei., "Kinematic Analysis of a Three Degrees of Freedom Spherical Wrist Actuator," *Proc. of the Fifth Int. Conf. on Advanced Robotics*, Italy, 1991.
- [9] Sciavicco, L. and Siciliano, B., *Modeling and Control of Robotic Manipulators*, McGraw-Hill: New York, 1996.

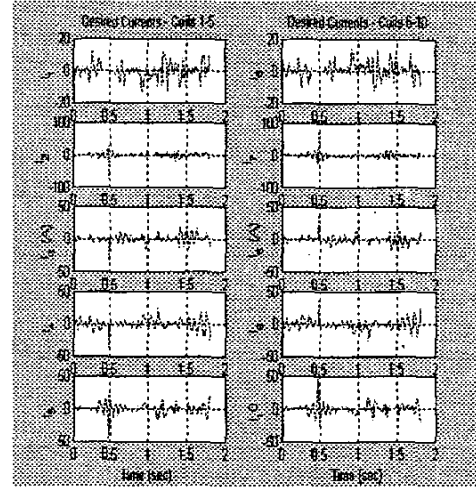


Figure 8(a) Desired Currents-(test case #2)

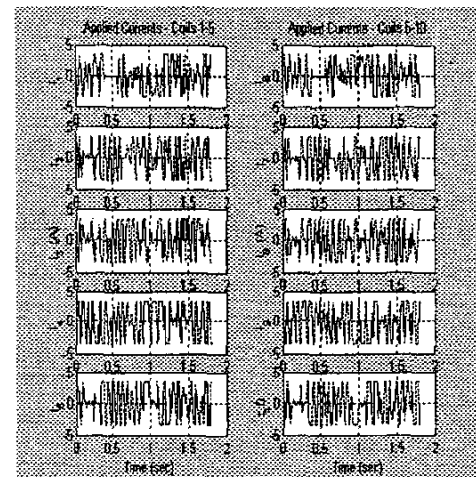


Figure 8(b): Applied currents

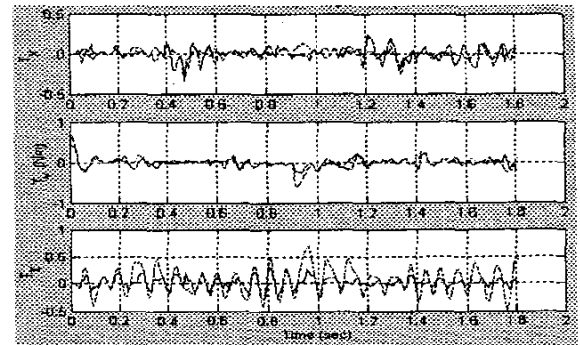


Figure 9: Desired and Applied Torque- (test case #2)